# Artifact Reduction in Electrogastrogram Based on the Empirical Mode Decomposition Method

**Hualou Liang, Zhiyue Lin *, Richard W. McCallum ***

Center for Complex Systems & Brain Sciences,
Florida Atlantic University,
777 Glades Road, Boca Raton, FL 33431

*University of Kansas Medical Center, Department of Medicine,
Kansas City, Kansas 66160

Corresponding author:

Hualou Liang, Ph.D.
Center for Complex Systems
Florida Atlantic University
777 Glades Road
P.O. Box 3091
Boca Raton, FL 33431, USA
Tel: 561-297-0108
Fax: 561-297-3634
E-mail: liang@walt.ccs.fau.edu

## Abstract

Severe contamination of gastric signal in the electrogastrogram (EGG) by respiratory, motion, cardiac signals, and possible myoelectrical activity from other organs poses a major challenge for EGG interpretation and analysis. The aim of this paper is to present a generally applicable method for removing a variety of artifacts from EGG recordings based on the Empirical Mode Decomposition (EMD) method. This decomposition technique is adaptive, and appears to be uniquely suitable for nonlinear, nonstationary data analysis. The performance of the proposed method was investigated using computer simulations. Based on the quantitative measure of the processed results we showed that the EMD method produced superior result compared to the conventional band-pass filtering. Experimental EGG data were obtained from both healthy subjects and patients with dyspeptic symptoms. Our results of real EGG data demonstrated that the proposed method yields efficient artifact reduction in the EGG and keeps the gastric signal less affected. These data suggest that the EMD method, while combined with instantaneous frequency analysis, can be used to separate, identify and remove contamination from a variety of artifactual sources in EGG recordings.



**keywords** Electrogastrogram, Empirical mode decomposition, Artifact reduction, Hilbert transform, Nonstationary.

# 1 Introduction

Since the landmark development of electrogastrogram (EGG) by Alvarez (1922), cutaneous EGG has been used as a non-invasive approach for physiological and pathophysiological studies of the stomach, and used as a clinical tool for the evaluation of gastric dysrhythmia (Chen and McCallum, 1991, 1993a). Ironically, after 70 years of research, severe contamination of gastric signal in the EGG by respiratory, motion, cardiac signals and possible myoelectrical activity from other organs remains a serious problem for EGG interpretation and analysis. So without appropriate artifact/noise reduction an EGG evaluation is almost impossible.

The electrical activity of the healthy stomach is mainly composed of rhythmic slow waves and spikes. The fundamental frequency of the gastric signal is around 3 cycles/min (3 cpm or 0.05 Hz) in healthy humans, but its waveform is not sinusoidal. This means that the gastric signal may have harmonics. Like the electrocardiogram (ECG), an EGG recording may consist of not only normal rhythms but also dysrhythmia including tachygastria, bradygastria and arrhythmia. In addition, the amplitude and frequency of the gastric signal component change from time to time (Chen and McCallum, 1993b). The frequencies of the ECG and respiratory artifact are about 1 Hz and 0.2-0.4 Hz, respectively. The frequency-domain filter could be applied to suppress the noise while preserving the gastric signal. This standard approach can be only as effective as the Fourier basis capable to separate signals from noise, which will hardly to be the case for broad-band signals, e.g. motion artifact. Moreover, since the electrical signal of stomach is not sinusoidal, conventional frequency-domain filtering may distort waveforms of the gastric signal by filtering out harmonics of the fundamental frequency of the gastric signal. Therefore, artifacts contaminated in EGG cannot be eliminated by using conventional frequency filtering without affecting the gastric signal.

Adaptive filtering technique (Chen and Lin, 1994) has been shown to improve the quality of the EGG or to extract relevant information from the EGG. An inherent weakness of this method, however, is requiring a reference signal that is the comprehensive signal of the various artifacts to be removed. Obviously, it is difficult and sometimes unrealistic to obtain such a reference signal in practical applications, because artifacts are variable, and their nature of distribution is unknown.

An attractive method (Liang et al., 1997) using feature analysis and neural networks has been reported to realize automatic detection and elimination of the motion artifacts in EGG recordings. In this method, once an EGG segment is detected as containing motion artifacts, the whole segment is deleted. In case limited data are available, or the motion artifacts occur too frequently, the amount of data lost to artifact rejection may be unacceptable.

We present here a generally applicable method for isolating, identifying and removing a wide variety of artifacts in the EGG using a newly-developed method – Empirical Mode Decomposition (EMD) (Huang et al., 1998a). This technique, while combined with the Hilbert transform, makes itself ideally suited for nonlinear and non-stationary data analysis. In this paper, we analyze the EGG data to demonstrate the effectiveness of this method.

# 2 Methods

## 2.1 The Empirical Mode Decomposition Method

The EMD method was initially proposed in the study of fluid mechanics (Huang et al., 1998a), and found immediate applications in biomedical engineering (Huang et al., 1998b). The central idea of this method is the sifting process to decompose any given signal into its fundamental modes, those basic building blocks that make up complicated data. If we were to apply a Fourier decomposition to the signal, then the basis functions are linear combinations of sine and cosine waves, which would be the case if the signal were linear. Fourier analysis therefore merely works well for strictly linear, stationary random functions of time. With the EMD approach, the basis functions themselves are nonlinear functions which can be extracted directly from the data, or in other words, an adaptive basis called Intrinsic Mode Function (IMF) can be found.

A signal must satisfy two criteria to be an IMF, the first one being that the number of local maxima and the number of local minima differ by at most one, and the second, the mean of its upper and lower envelopes equals zero.

Given these two definitive requirements of an IMF, the problem of interest is how we derive an IMF from a given data $X(t)$, e.g. EGG recording, as shown in Fig. 1(a) in thin solid line. The solution essentially consists of three major steps:

*step 1:* we construct two smooth splines connecting all the maxima and minima of $X(t)$ to get its upper envelope, $X_{up}(t)$, and its lower envelope, $X_{low}(t)$, which are plotted with dotted lines in Fig. 1(a); The extrema can be simply found by differentiation of the data sampled at discrete points and then determine where the sign flips. Once the extrema are identified, all the maxima are connected by cubic spline line as the upper envelope. Repeat the procedure for the local minima to produce the lower envelope. The upper and lower envelopes should cover all the data between them.

*step 2:* we subtract the mean of these two envelopes from the data to get their difference $X_1(t)$,

$$X_1(t) = X(t) - (X_{up} + X_{low})/2; \tag{1}$$

In Fig. 1(a) we plot the mean of envelopes in thick solid line.

*step 3:* we repeat steps (1) and (2) for $X_1(t)$ until the resulting signal meets the the criteria of an intrinsic mode.

These three steps give the general scenario of the sifting process. We can see that the signal $X_1(t)$, as shown in Fig. 1(b) with thin solid line, is not an IMF, for there are a few negative local maxima and positive minima. This situation is improved by two more interactions, as shown in Fig. 1(c), the mean is still not zero. Keep iterating, the convergent signal denoted as $C_1(t)$, Fig. 1(d), is the first IMF of data $X(t)$, which has a zero local mean.

We then treat the residue $R_1(t) = X(t) - C_1(t)$ as new data that are subject to the sifting process as described above, yielding the second IMF from $R_1(t)$. The procedure continues until finally a mode becomes less than a predetermined small number or the residue becomes non-oscillatory. The original signal $X(t)$ can thus be expressed as follows:

$$X(t) = \sum_{j=1}^{N} C_j(t) + R_N(t), \tag{2}$$

where $N$ is the number of IMFs, $R_N(t)$ is the final residue which can be either the mean trend or a constant, and functions $C_j(t)$ are nearly orthogonal to each other, and all have zero means. By the nature of the decomposition procedure, the technique decomposes data into $N$ fundamental components, each with distinct time scale. More specifically, the first component has the smallest time scale which corresponds to the fastest time variation of data. As the decomposition process proceeds, the time scale increases, and hence, the mean frequency of the mode decreases. Since the decomposition is based on the local characteristic time scale of the data to yield adaptive basis, it is applicable to nonlinear and non-stationary data in general and in particular, EGG data considered in the following section.

## 2.2 The Hilbert Transform

Once all the IMFs' are found, the instantaneous frequency of each component can be readily obtained by utilizing the Hilbert transform, which can be used later for signal identification.

The Hilbert transform has been widely used in order to obtain the analytic signal associated with the real signal $x(t)$, and, consequently, its instantaneous envelope and phase functions. The instantaneous frequency which is of interest in our present report can be further derived from the instantaneous phase, and its definition is given below (Oppenheim and Schafer, 1975).

Given a time series $x(t)$, the corresponding analytic signal is defined to be

$$z(t) = x(t) + iH[x(t)] = a(t)\exp[i\theta(t)], \tag{3}$$

where the $a(t)$ and $\theta(t)$ are the instantaneous amplitude and phase of the analytic signal $z(t)$, and the imaginary part $H[x(t)]$ is the Hilbert transform of $x(t)$:

$$H[x(t)] = \mathcal{P}[\frac{1}{\pi}\int_{-\infty}^{\infty}\frac{x(u)}{t-u}du].$$

Here, the notion $\mathcal{P}$ indicates the Cauchy principal value of the integral (Oppenheim and Schafer, 1975). If $\mathcal{F}\{x(t)\}$ and $\mathcal{F}\{z(t)\}$ are respectively the Fourier transforms of $x(t)$ and $z(t)$, then the above relationship is expressed in the frequency domain by

$$\mathcal{F}\{z(t)\} = \begin{cases} 2\mathcal{F}\{x(t)\} & \text{if } \omega > 0, \\ \mathcal{F}\{x(t)\} & \text{if } \omega = 0, \\ 0 & \text{if } \omega < 0 \end{cases} \tag{4}$$

Thus, the analytic signal, which still retains the information content of its original real signal, can be obtained from Eq. 4. With the instantaneous phase, it is then possible to define in a unique way the concept of instantaneous frequency by

$$\omega(t) = d\theta(t)/dt \tag{5}$$

By virtue of the analytic signal, the given signal can be faithfully represented by the amplitude and the frequency as functions of time in a three-dimensional plot, in which the amplitude distribution on the time-frequency plane is referred to as the Hilbert spectrum.

# 3 Experimental Results

The artifact reduction procedure consists of three major steps. **The first step** is to decompose the data into a number of IMF components by the empirical mode decomposition. **The second step** is to perform the Hilbert transform to each of the IMF components to obtain its instantaneous frequency. **The final step** is to identify the artifactual or relevant signals on the basis of prior knowledge, and then extract cleaner EGG.

A validation study is first performed to test the efficiency and performance of the artifact reduction method. Then, two sets of EGG data, each from different subject, are selected to illustrate the application procedure of the EMD method. Followed is the extraction of gastric slow waves using this method from an EGG recording with motion interference.

## 3.1 Validation

Computer simulations have been conducted to evaluate the performance of the proposed artifact reduction method. The simulated EGG signal (Fig. 2(c)) was composed of a pure gastric electrical signal (Fig. 2(a)), a respiratory and motion artifacts (Fig. 2(b)) and white noise. The pure gastric electrical signal was obtained from a pair of serosal electrodes in a patient. The respiratory and moton artifacts were obtained using a pneumatrace belt. The EMD method yields eight IMF components as shown in Fig. 3. The instantaneous frequencies of these IMF components by using Hilbert transform are given in Fig. 4, in which the third and second component are the gastric signal and its harmonic, the first component should be respiratory artifact. The extracted gastric signal (component 2 and 3) is presented in Fig. 2(d). For comparison, the result of band-pass filtering with low and high cut-off frequencies of 0.5 and 6 cpm, respectively is shown in Fig. 2(e). It is evident from Fig. 2 that the EMD method produces superior result. It is more intuitive to examine their Fourier spectra as shown in Fig. 5, in which the spectra of the mixed signal, the pure gastric signal, the extracted gastric signal by the EMD method and that by conventional band-pass filtering are shown in dashed, dotted, thick solid and thin solid lines, respectively. We can see from these curves that the spectrum of the extracted gastric signal by the EMD method is slightly different from that of the pure gastric signal, whereas the conventional band-pass filtering results in large deviation, particularly at the high frequency range.

To quantify the performance of EMD method, the following relative error is defined:

$$\delta = \frac{\sum_f [P(f) - P'(f)]^2}{\sum_f P^2(f)}$$

where $P(f)$ is the spectral density of the pure gastric signal and $P'(f)$ is the spectral density of the extracted or filtered gastric signal, $f$ ranges from 0.5 to 9 cpm. Indeed, the EMD yields smaller relative error (0.0595) than that of conventional band-pass filtering (0.1514).

## 3.2 Applications to EGG Recording

The EGG data used in this study were obtained from both healthy subjects and patients with dyspeptic symptoms by using a portable EGG recorder (Synectics, Irving, TX) with low and high cut-off frequencies of 1.0 and 18.0 cpm, respectively. Three silver/silver chloride electrodes (VER MED, Bellow Falls, VT) were placed on the abdominal skin over the stomach. Two epigastric electrodes were connected to yield a bipolar EGG signal, one electrode at the midpoint between the xiphoid and the navel, and the other at 5 cm to the left and 5 cm above this point. The third electrode, placed at the left costal margin horizontal to the first electrode, was used as a reference. The signal was on-line digitized at a sampling frequency of 1 Hz.

In the first application, a 10-min EGG recording from a healthy subject, as shown in Fig. 6(a), was used in the experiment. Fig. 7 shows the resulting IMF components. The Hilbert transforms of these IMF components give their instantaneous frequencies shown in Fig. 8. The first three components correspond to heart beating, respiratory artifact and harmonic signal respectively. Component 4 should be the ongoing gastric slow wave around 3 cpm which clearly reflects the non-stationary nature of gastric activity.

It is even more convinced by scrutinizing its frequency content of each component, as shown in Fig. 9. The peak frequencies of component 1, 2, 3 and 4 are successively 1.02 Hz, 0.2 Hz, 0.1 Hz and 0.05 Hz, which correspond to heart beating, respiratory artifact, harmonic signal and gastric slow wave, respectively. For comparison, we plot the extracted gastric signal (Component 3 and 4) in Fig. 6(b). The frequency contents of the original EGG and extracted gastric signal are shown in Fig. 6(c). We can observe from these figures that the gastric signal component is effectively extracted whereas other noise and artifacts are greatly reduced.

In the second application, we use an EGG recording from a patient with dyspeptic symptoms. Fig. 10(a) shows a 10-min EGG signal. These data, when subjected to the empirical mode decomposition method, yielded seven components and a residue, as shown in Fig. 11. The residue obviously should be the DC component or the trend in the data, a further benefit from EMD method. The instantaneous frequencies of the IMF components are presented in Fig. 12, in which the frequency of the first two components fluctuating over a considerable range at 0.14 Hz corresponds to respiratory artifact. The resulting signal in the time domain after removing the first two IMF components and the DC component as well is shown in Fig. 10(b). The Fourier spectra of the extracted and orginal signals are shown in Fig. 10(c), from which we can see that both high frequency and DC components are effectively reduced. What left is dominated by bradygastria with a frequency of less than 1.5 cpm.

To further illustrate the effectiveness of the EMD method, we select a 10-min EGG recording with heavy motion interference, a more difficult case of artifact removal. In contrast to the aforesaid examples, we can see from the EGG recording as shown in Fig. 13(a), the weak gastric signal is mostly submerged in the motion artifacts, therefore, it is necessary to firstly use proper preprocessing method to weaken the power of motion interference, and then apply the EMD method. To tackle this thorny problem, we devised a preprocessing procedure by thresholding the raw EGG data $x(t)$ according to the following formula:

$$x(t) = \begin{cases} p1 & \text{if } x(t) > p1, \\ p2 & \text{if } x(t) < p2, \\ x(t) & \text{others} \end{cases}$$

where $p1, p2$, the applied thresholds as plotted in Fig. 13(a) in dashed lines, are respectively the mean $\pm$ 3 $\times$ (standard deviation) of the EGG segment without severe motion artifacts. By comparison of the power spectra of before (in thin solid line) and after (in dotted lines)thresholding the EGG data, as shown in Fig. 13(c), the power of EGG data is not or less affected. More sophisticated preprocessing method, of course, can be done by applying the adaptive thresholding approach (Donoho and Johnstone, 1995). However, we found this method is adequate for our purpose.

Following the empirical mode decomposition and signal identification procedure as stated above, the IMF components of the preprocessed EGG is presented in Fig. 14. The extracted gastric signal (component 4) is shown in Fig. 13(b), and its power spectrum is plotted in Fig. 13(c) in thick solid line. It is clearly observed that the motion artifacts and high frequency components in the EGG recording are greatly reduced.

# 4 Discussion and Conclusions

A newly-developed signal processing method - EMD is introduced and its successful applications in artifact reduction in cutaneous EGG are presented in this paper.

EGG is a cutaneous measurement of electrical activity of the stomach. It is very attractive because it is non-invasive and does not disturb the ongoing activities of the stomach. Unlike other surface electrophysiological measurements such as electrocardiography (ECG), however, the clinical applications of this non-invasive method have been limited (Chen and McCallum, 1993a). One of the main problems with the EGG is the poor quality of the recording, i.e., the weakness of the real gastric signal and the heavy interference such as ECG, respiratory and motion artifacts. As a result, direct visual analysis of the EGG is impossible. Several methods have been designed and applied to improve the quality of the EGG including bandpass filtering (Nelsen and Kohatsu, 1968; Stoddard et al., 1981), fast Fourier transform (Brown et al., 1975; van der Schee and Grashuis, 1987), phase-lock filtering (Smallwood, 1978), autoregressive modeling (Linkens and Datardina, 1978), adaptive filtering (Chen and Lin, 1994) and neural networks (Liang et al. 1997). Although each of these methods has its advantages over the others, they only have limited success in practical applications. This is because there are some crucial restrictions for all the above methods: *linearity* of the system and *stationarity* of the data. It has been already proved that the amplitude and frequency of gastric signal in the EGG may change over time and these changes are non-stationary (Lin and Chen, 1994, 1995; Chen et al. 1993b). In addition, it has been also shown that an EGG signal has a chaotic behavior with a strange attractor (Lindberg, 1996). Therefore, an advanced method for processing nonlinear and non-stationary signals is needed to improve the quality of the EGG.

The EMD method (Huang et al., 1998a) introduced in this paper decomposes any given data into a finite and often small numbers of IMFs that admit well-behaved Hilbert transforms. With the EMD approach, the basis functions used to represent the given signal are nonlinear functions which can be extracted directly from the data. In other words, an adaptive basis called IMF can be found. Since the decomposition is based on the local characteristic time scale of the data to yield the adaptive basis, the EMD method is applicable to nonlinear and non-stationary processes. As stated above, both the gastric signal and artifacts in the EGG may be non-stationary and therefore the EMD method is well suited for processing the EGG. Another advantage of this method is that the decomposition components usually have more physically meaningful interpretation of the underlying dynamic processes. To identify the artifacts and gastric signal in the EGG, the next step is to perform the Hilbert transform to each of the decomposed IMF components to obtain their instantaneous frequencies. Based on the prior knowledge about the frequency rang of the gastric signal, it is easy to extract the clean gastric signal from the IMF components of the EGG data. Experiments on real EGG data showed that the EMD method does yield more efficient artifact reduction in the EGG and keep the gastric signal less affected.

There is much room for improvement in the EMD method. The spline fitting is the essential step in generating the IMF. Although the present envelope-mean method works well in most cases, problems still exist. The cubic spline fitting adopted here has both overshoot and undershoot problems. These problems can be alleviated by using more sophisticated spline methods, such as the higher-order spline program. However, such improvement would probably be marginal. It should be indicated that an additional step may have to be taken to preprocessing the EGG data before the use of EMD method when the the gastric signal embedded in stronger motion artifacts. This is because the EMD method is build on the identification of scale from successive of extrema (Huang et al., 1998a). If the gastric signals are phase locked with, and occur only at the maximum slope regions of the strong motion artifacts, then it will be difficult to recover the gastric signal. In this case, either a hard-threshold or differentiation of original data could be used before using the EMD method. It is also worth noting that the EMD method is effective use of the data, which is particularly useful where only limited data is available.

In conclusion, this paper has shown that the EMD method combined with instantaneous frequency analysis is powerful and very useful in removing artifacts in cutaneous EGG recording.

# References

Alvarez, W.C. (1922): 'The electrogastrogram and what it shows', *J. Amer. Med. Assoc.*, **78**, pp. 1116-1118

Brown, B.H. Smallwood, R.H, Duthie H.L., and Stoddard, C.J. (1975): 'Intestinal smooth muscle electrical potentials recorded from surface electrodes',*Med. & Biol. Eng.*, **13**, pp. 97-103

Chen, J., McCallum, R.W. (1991): 'Electrogastrogram: Measurement, Analysis and Prospective Applications', *Med. Biol. Eng. Comput.*, **29**, pp. 339-350

Chen, J.D.Z. and McCallum, R. W. (1993a): 'Clinical application of electrogastrogram', *Am. J. Gastroenterol.*, **88**, pp. 1324-1336

Chen, J., Stewart, W.R. and McCallum, R.W. (1993b): 'Adaptive spectral analysis of episodic rhythmic variations in the cutaneous electrogastrogram', *IEEE Trans.*,**BME-40**, pp. 128-135

Chen, J., and Lin, Z.Y. (1994): 'Comparison of Adaptive Filtering in Time-, Transform- and Frequency-Domain: An Electrogastrographic Study', *Ann. Biomed. Eng.*, **22**, pp. 423-431

Donoho, D., and Johnstone, I. (1995): 'Adapting to unknown smoothness via wavelet shrinkage', *J. Am. Stat. Assoc.*, **90**, pp. 1200-1224

Huang, N.E., Shen, Z., Long, S.R., Wu, M.L.C., Shih, H.H., Zheng, Q.N., Yen, N.C., Tung, C.C. and Liu, H.H. (1998a): 'The empirical mode decomposition and the Hilbert spectrum for nonlinear and non-stationary time series analysis', *Proc. Roy. Soc. LOND A MAT*, **454**, pp. 903-995

Huang, W., Shen, Z., Huang, N.E. and Fung, Y.C. (1998b): 'Engineering analysis of biological variables: An example of blood pressure over 1 day', *Proc. Nat. Acad. Sci. USA*, **95**, pp. 4816-4821

Liang, J., Cheung, J.Y., Chen, J.D.Z. (1997): 'Detection and deletion of motion artifacts in electrogastrogram using feature analysis and neural networks', *Ann.*

*Biomed. Eng.*, **25**, pp. 850-857

Lin, Z.Y., Chen, J. (1994): 'Time-Frequency Representation of the Electrogastrogram - Application of the Exponential Distribution', *IEEE Trans.* **BME-41**, pp. 267-275

Lin, Z.Y., Chen, J. (1995): 'Comparison of Three Running Spectral Analysis Methods for Electrogastrographic Signals', *Med. Biol. Eng. Comput.*, **33**, pp. 596-604

Lindberg, G. (1996): 'Is the electrogastrogram a chaotic parameter?', *Gastroenetrology*, **110** p. A707

Linkens, D.A. and Datardina, S.P. (1978): 'Estimation of frequencies of gastrointestinal electrical rhythms using autoregressive modeling', Med. & Biol. Eng. & Comput., **16**, pp. 262-268

Nelsen, T.S. and Kohatsu, S. (1968): 'Clinical electrogastrography and its relationship to gastric surgery', **Am. J. Surg.**, 116, pp. 215-222

Oppenheim, A. and Schafer, R. (1975): Digital Signal Processing. Prentice-Hall, New-Jersey.

Smallwood, R.H. (1978): 'Analysis of gastric electrical signals from surface electrodes using phase-lock techniques', Med. & Biol. Eng. & Comput., **16**, pp. 507-518

Stoddard, C.J., Smallwood, R.H. and Duthie, H.L. (1981): 'Electrical arrhythmias in the human stomach,' *Gut*, **22**, pp. 705-712

van der Schee, E.J. and Grashuis, J.L. (1987): "Running spectrum analysis as an aid in the representation and interpretation of electrogastrographic signals', Med. & Biol. Eng. & Comput., **25**, pp. 57-62

## Figure Captions

Figure 1: Illustration of the sifting processes: (a) the original data in thin solid line, with the upper and lower envelopes in dotted lines and the mean plotted in thick solid line; (b) the difference $X_1(t)$, the envelopes of maxima and minima and their mean; (c) results shown after two iterations; (d) the final IMF is shown.

Figure 2: Signals used in the simulation and the extracted clean EGGs by the EMD method and the conventional band-pass filtering: (a) a pure gastric signal obtained from serosal electrodes in a patient; (b) the respiratory and motion artifact; (c) the simulated EGG: the mixture of signal in (a) and (b), together with white noise; (d) the extracted clean EGG by the EMD method; (e) the extracted EGG by the band-pass filtering.

Figure 3: The eight IMF components of the simulated EGG in Fig. 2(c) obtained by the EMD method.

Figure 4: The instantaneous frequencies of the IMF components in Fig. 3.

Figure 5: The comparison of power spectra of the mixed signal (dashed line), the pure gastric signal (dotted line), the extracted gastric signal by the EMD method (thick solid line) and that by conventional band-pass filtering (thin solid line).

Figure 6: A typical EGG recording from one healthy subject before and after artifact reduction and their power spectra: (a) the original signal; (b) the extracted clean EGG; (c) the power spectra of signals in (a) (dot-dashed line) and (b) (solid line).

Figure 7: The IMF components from the EGG data in Fig. 6(a).

Figure 8: The instantaneous frequencies of the IMF components in Fig. 7. There

is considerable frequency variation, an indication that the EGG is not stationary.

Figure 9: The power spectra of the first four IMF components, where the peak frequency in each subplot is 1.02 Hz, 0.2 Hz, 0.1 Hz and 0.05 Hz respectively, which in turn correspond to heart beating, respiratory artifact, harmonic signal and gastric slow wave.

Figure 10: An EGG recording measured from a patient with dyspeptic symptoms before and after artifact reduction and their power spectra: (a) the original signal; (b) the extracted clean EGG after removing the first two IMFs and the DC component; (c) the power spectrum of clean EGG (solid line) in comparison with that of the original signal (dot-dashed line).

Figure 11: The resulting empirical mode decomposition components from the EGG signal in Fig. 10(a). Notice the last component, c8, is not an IMF; it is the trend.

Figure 12: The instantaneous frequencies of the IMF components in Fig. 11.

Figure 13: An EGG recording with motion artifacts before and after artifact reduction and their power spectra: (a) the original EGG recording, two dashed lines are the applied thresholds, discarding the values exceeding these limits; (b) the extracted clean EGG after removing the first two IMFs and the DC component; (c) the power spectrum of clean EGG (in thick solid line) in comparison with those of the original EGG data (in thin solid line) and preprocessed one (in dashed line), where the difference between the latter two is almost indiscernible implies that the gastric signal embedded in the EGG is not or less affected by our preprocessing procedure.

Figure 14: The nine IMF components obtained by the EMD method.

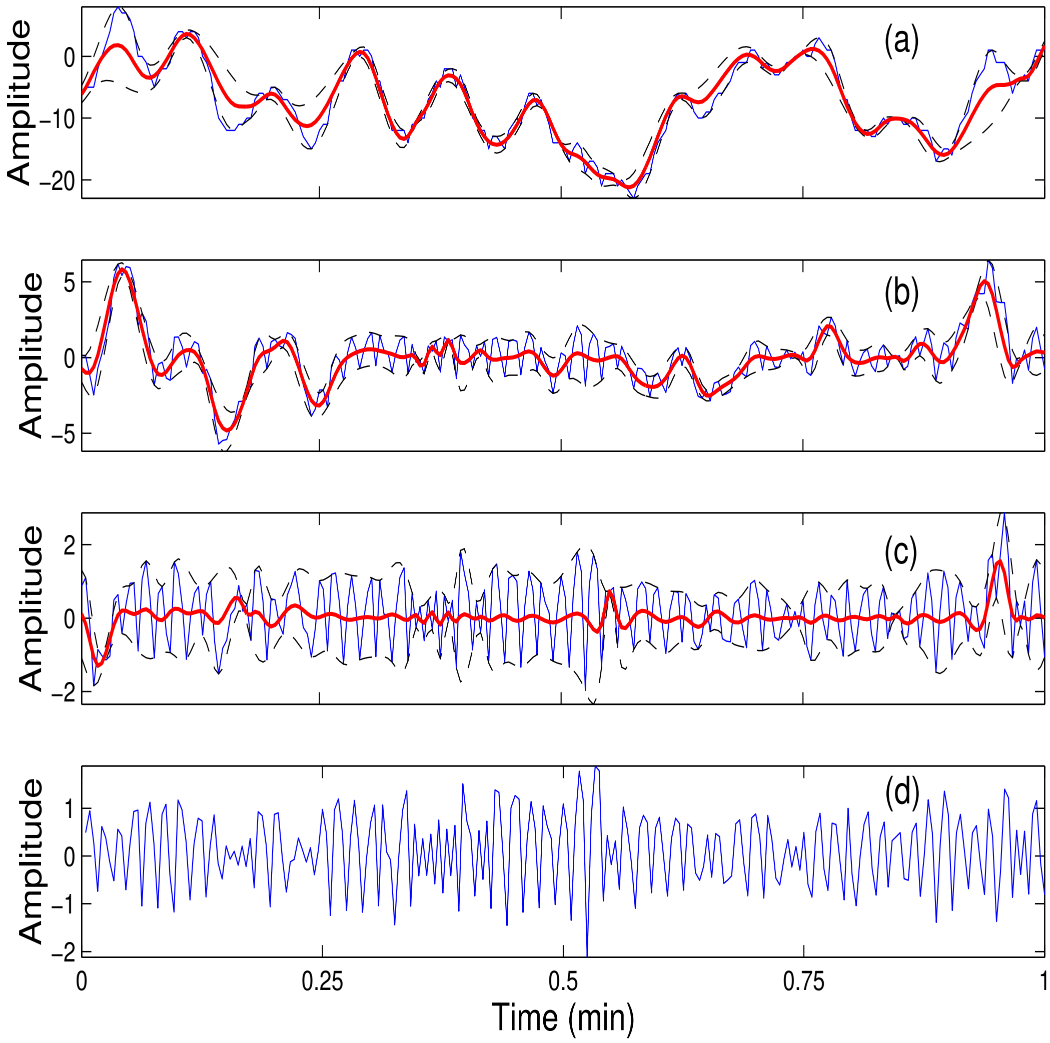


Figure 1

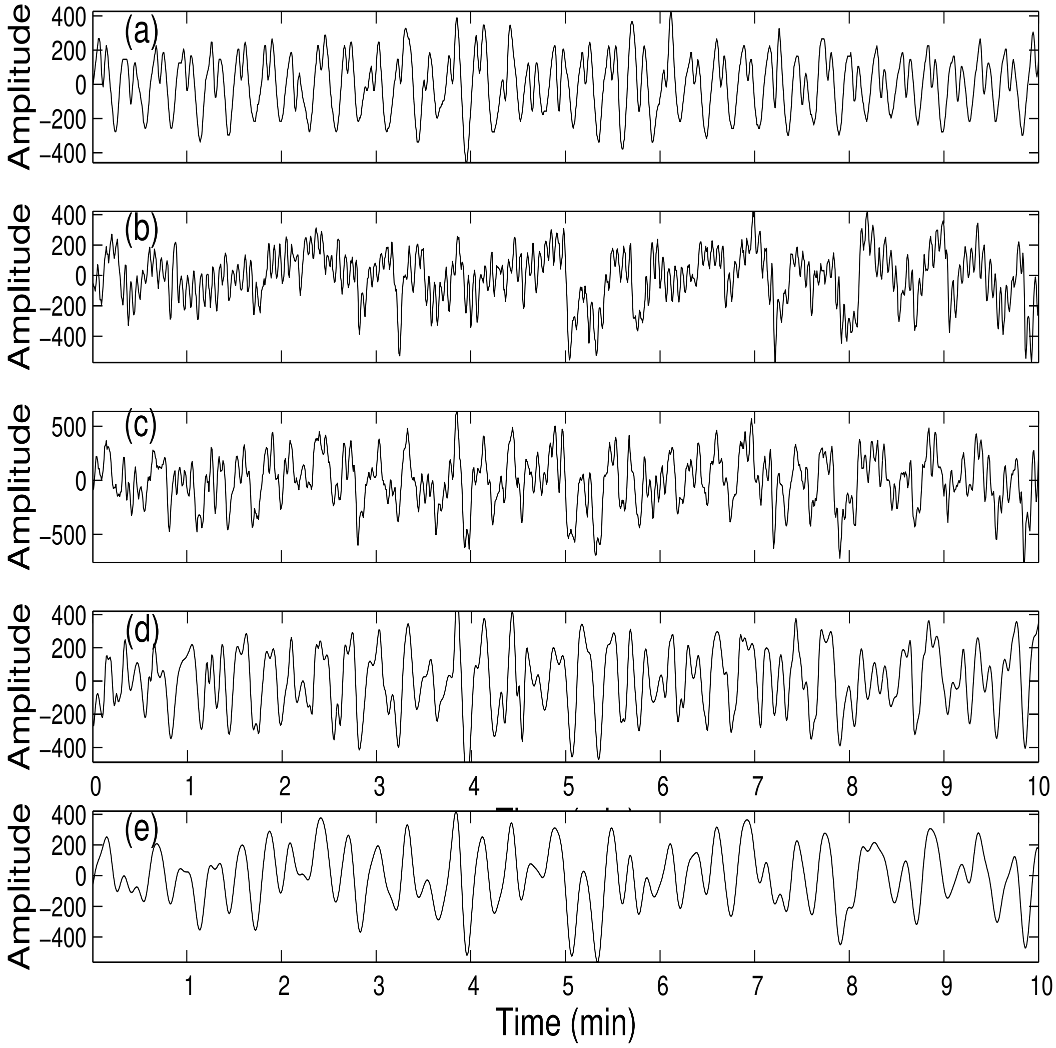

Amplitude
400
200
0
−200
−400
(a)
(b)
500
−500
(c)
(d)
(e)
0
1
2
3
4
5
6
7
8
9
10
Time (min)


Figure 2

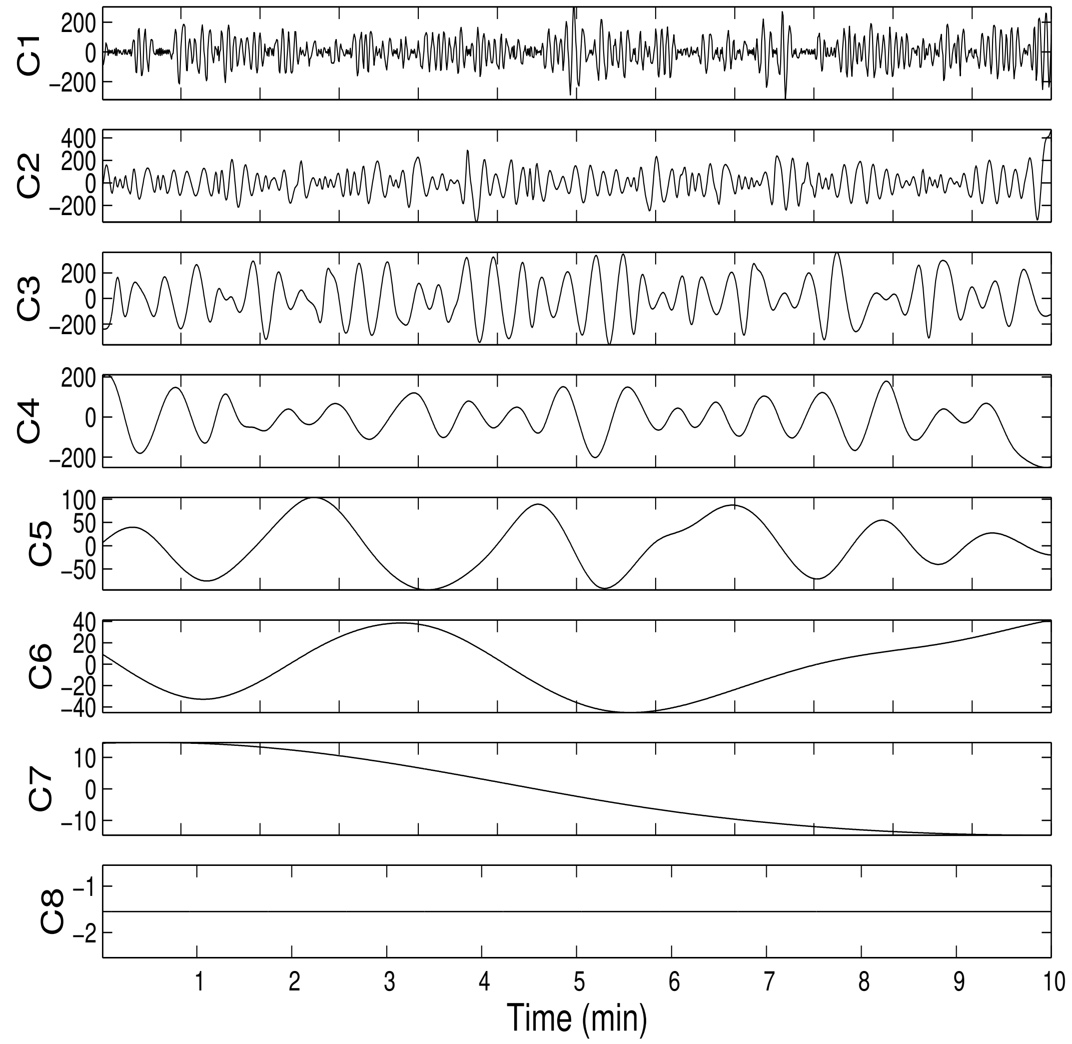
C1
200
0
−200
C2
400
200
0
−200
C3
200
0
−200
C4
200
0
−200
C5
100
50
0
−50
C6
40
20
0
−20
−40
C7
10
0
−10
C8
−1
−2
1
2
3
4
5
6
7
8
9
10
Time (min)

Figure 3

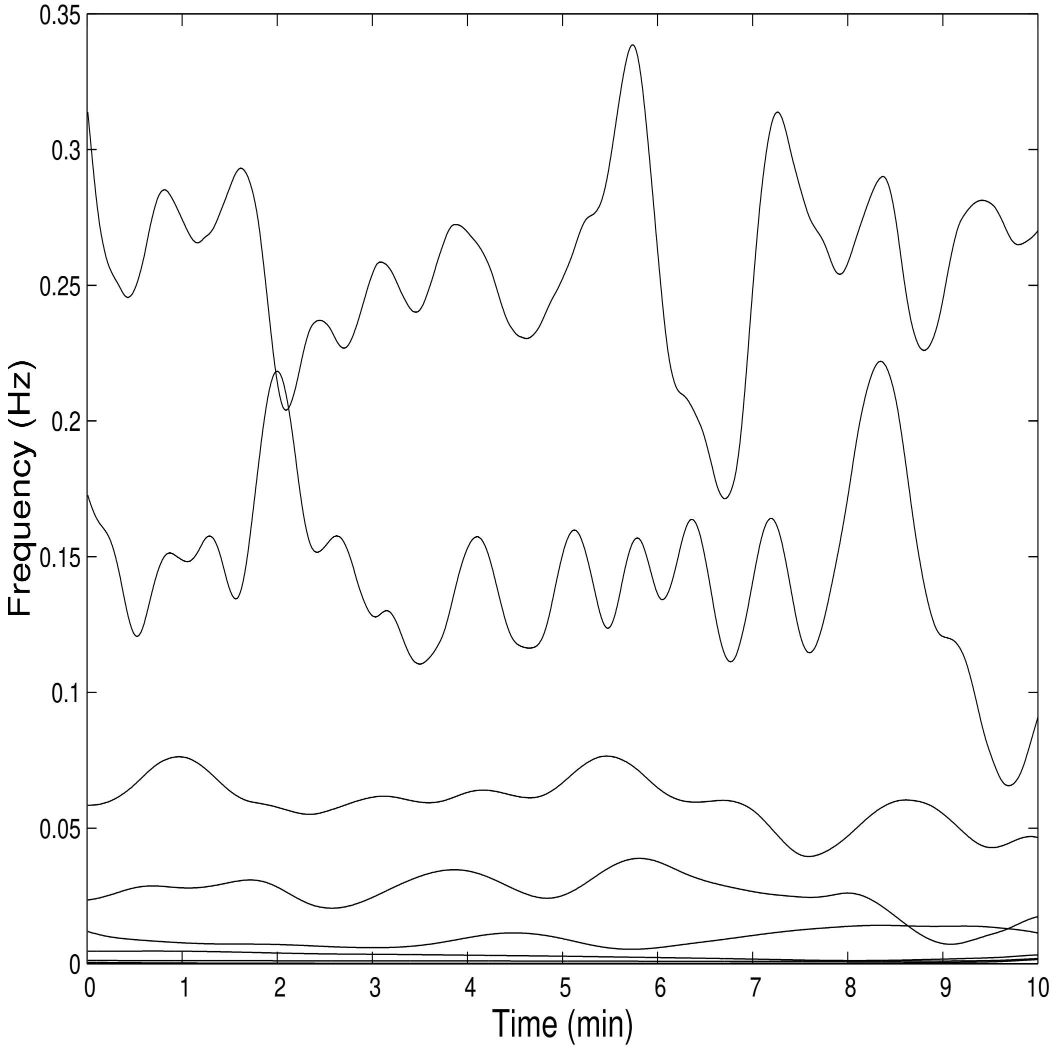


Figure 4

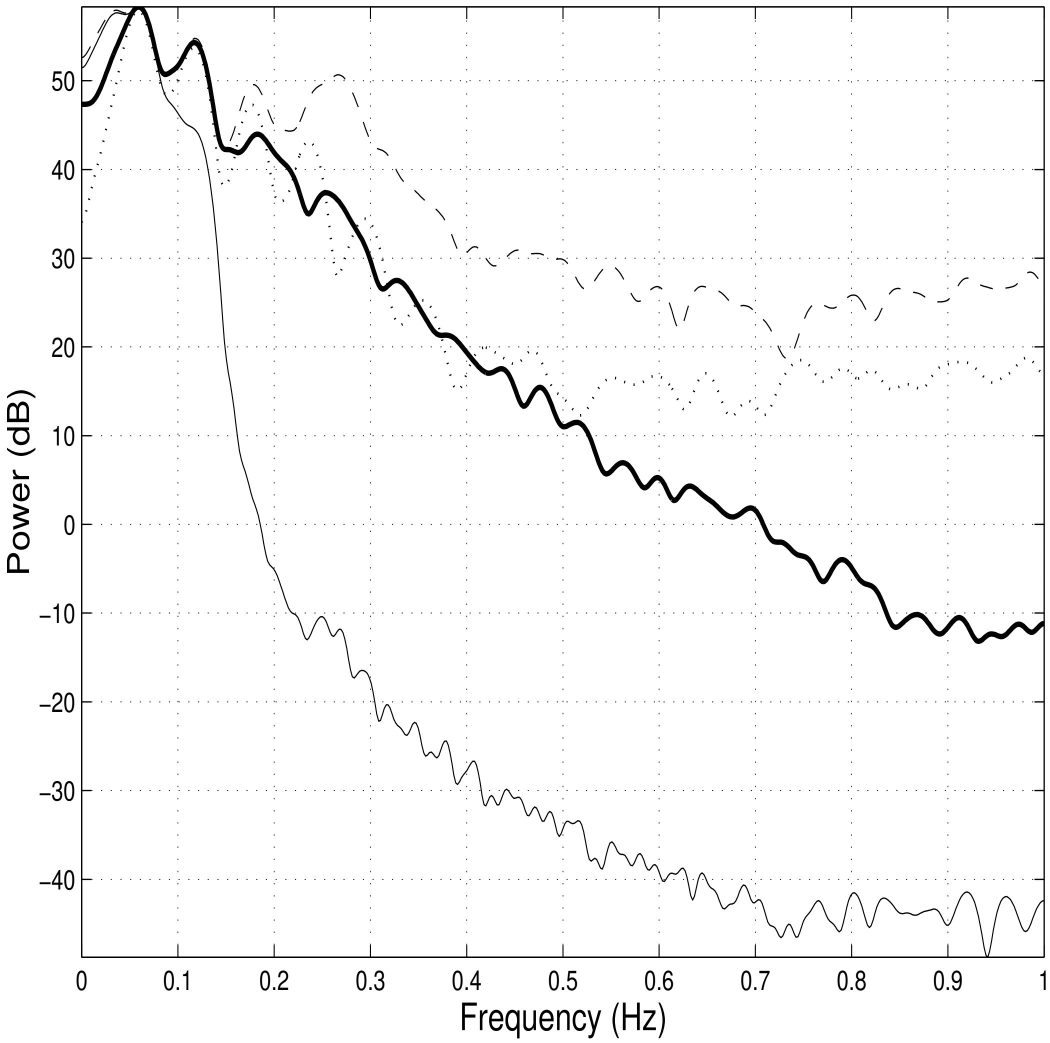
50
40
30
20
10
0
−10
−20
−30
−40
Power (dB)
0
0.1
0.2
0.3
0.4
0.5
0.6
0.7
0.8
0.9
1
Frequency (Hz)

Figure 5

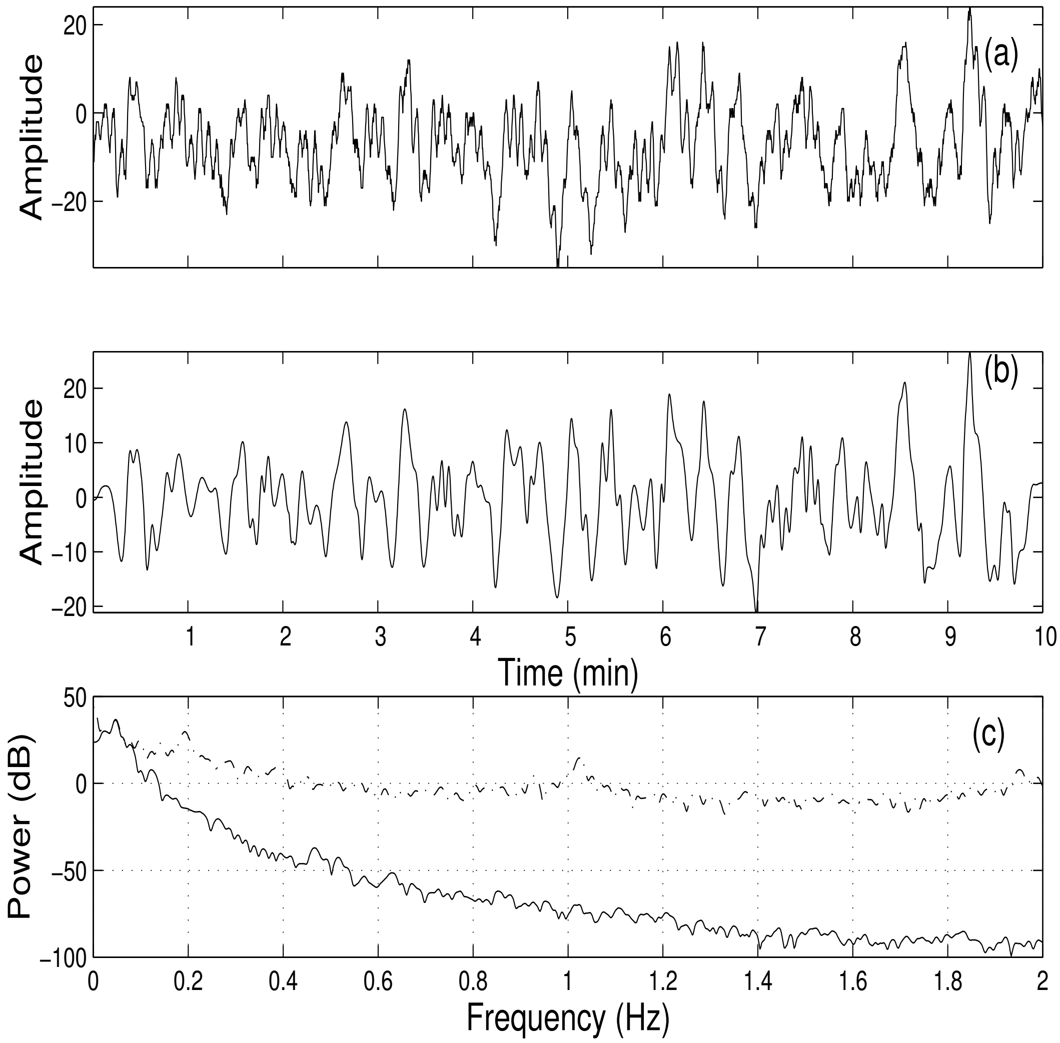


Figure 6

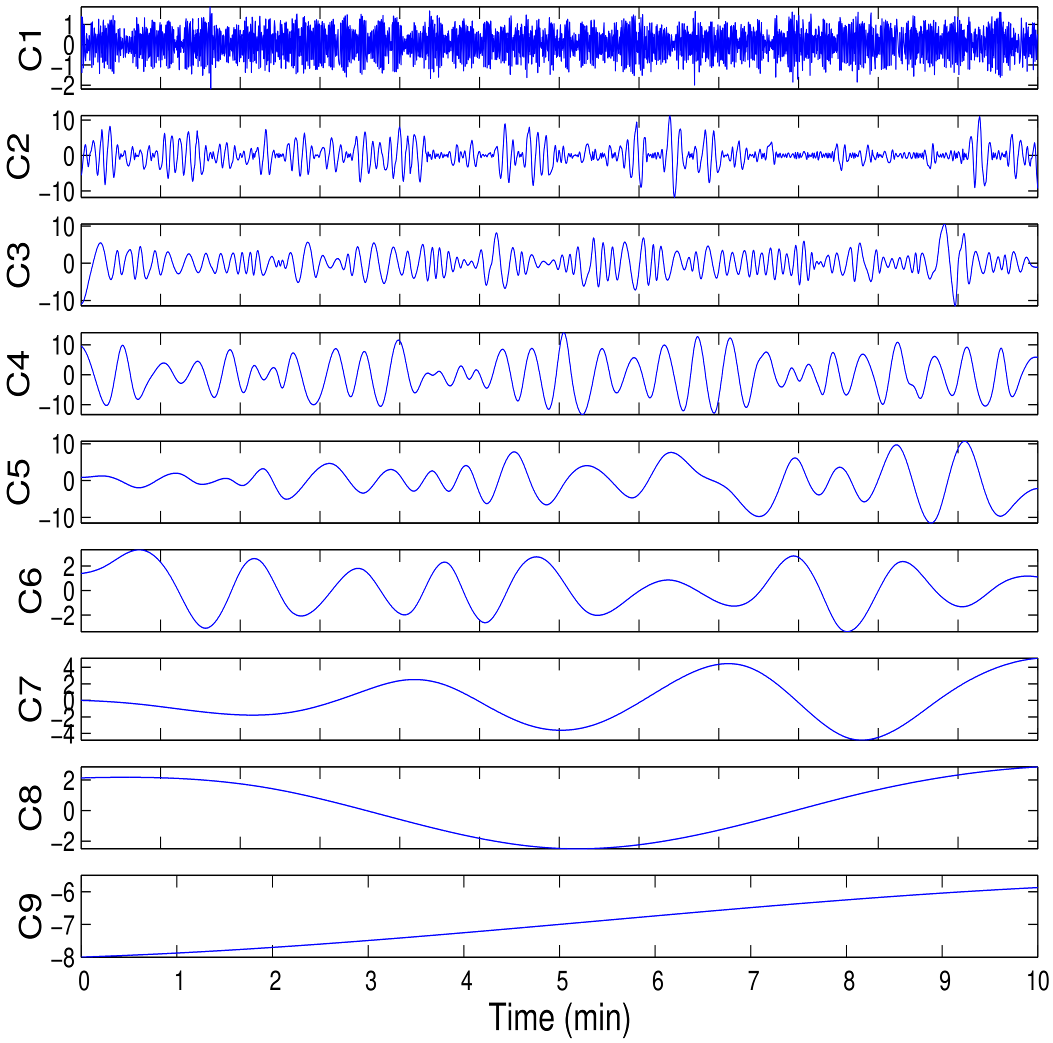


Figure 7

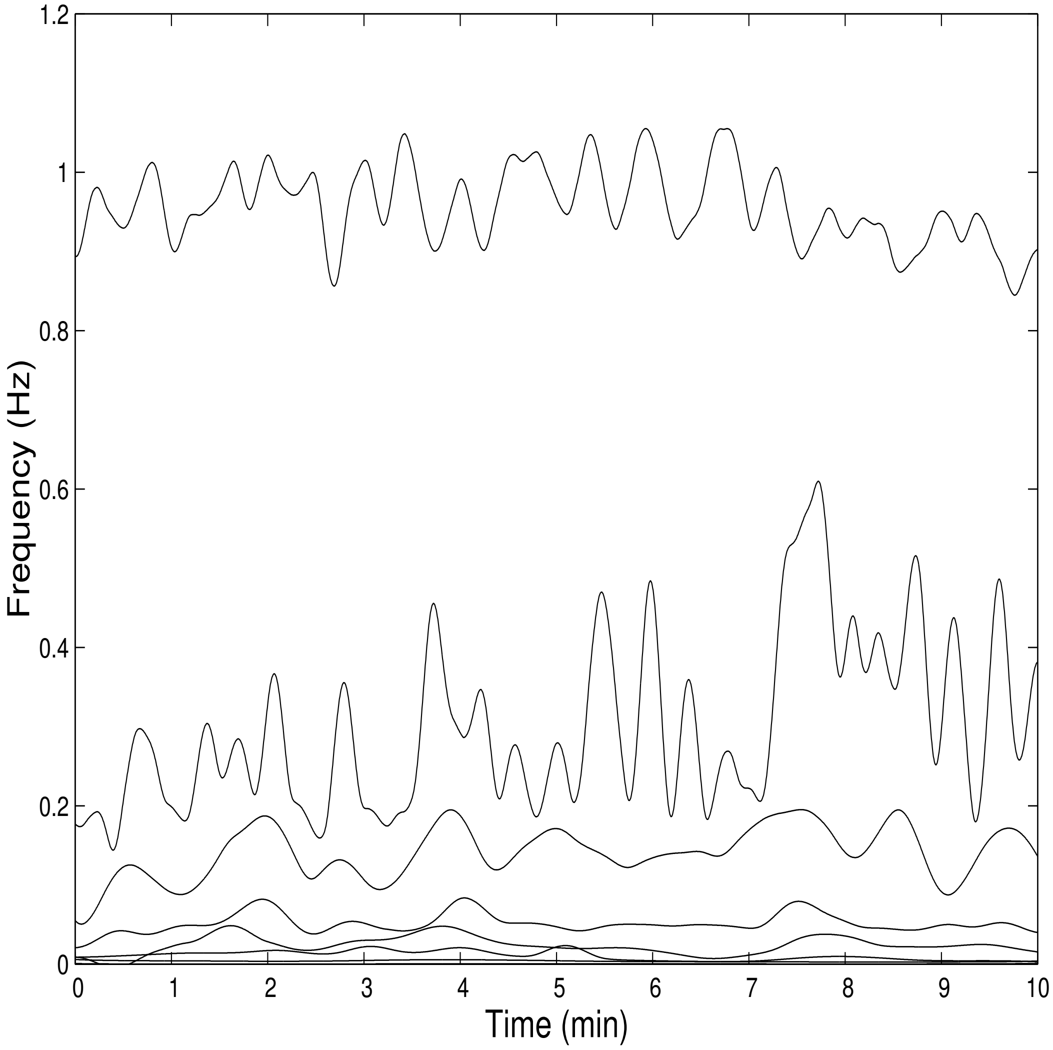


Figure 8

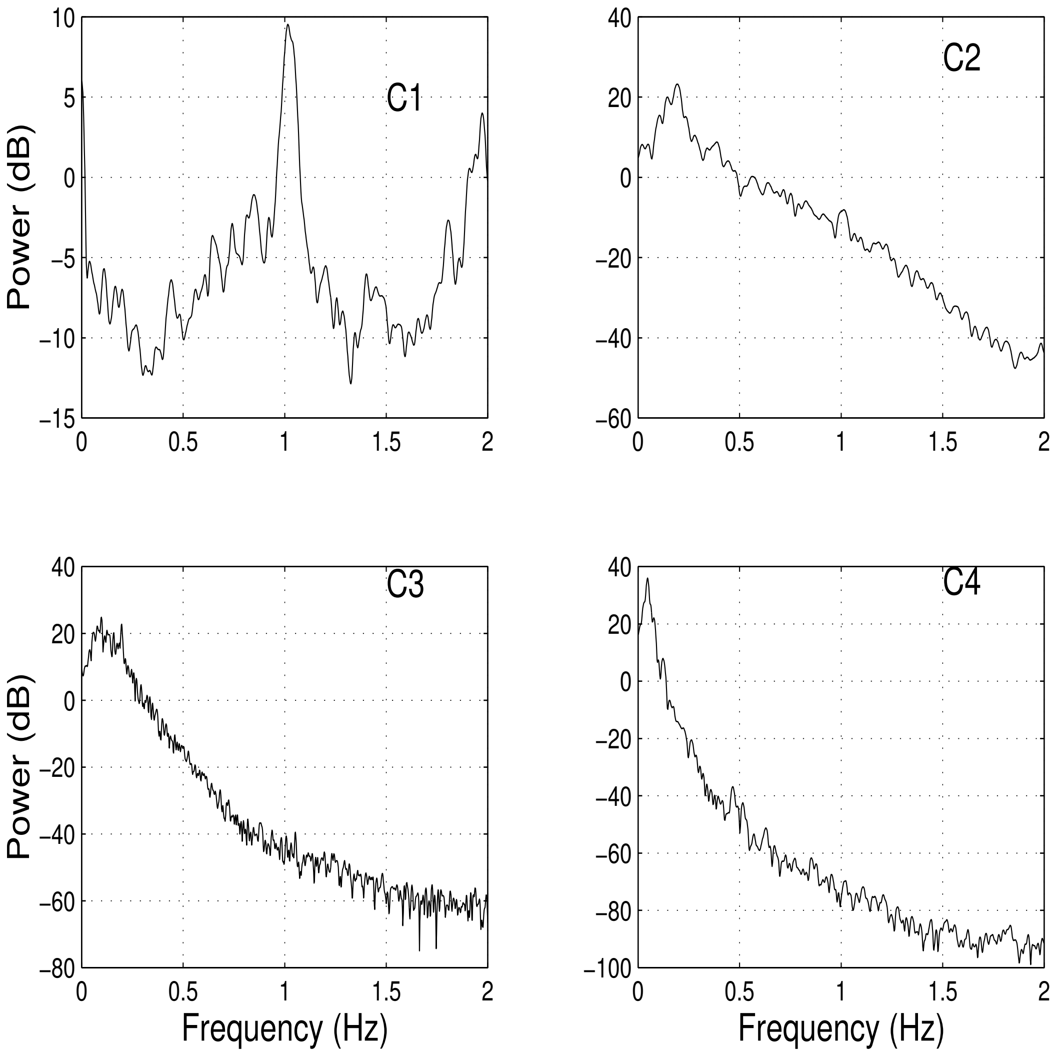
C1
C2
C3
C4
Power (dB)
Power (dB)
Frequency (Hz)
Frequency (Hz)
10
5
0
−5
−10
−15
40
20
0
−20
−40
−60
−80
−100
0
0.5
1
1.5
2

Figure 9

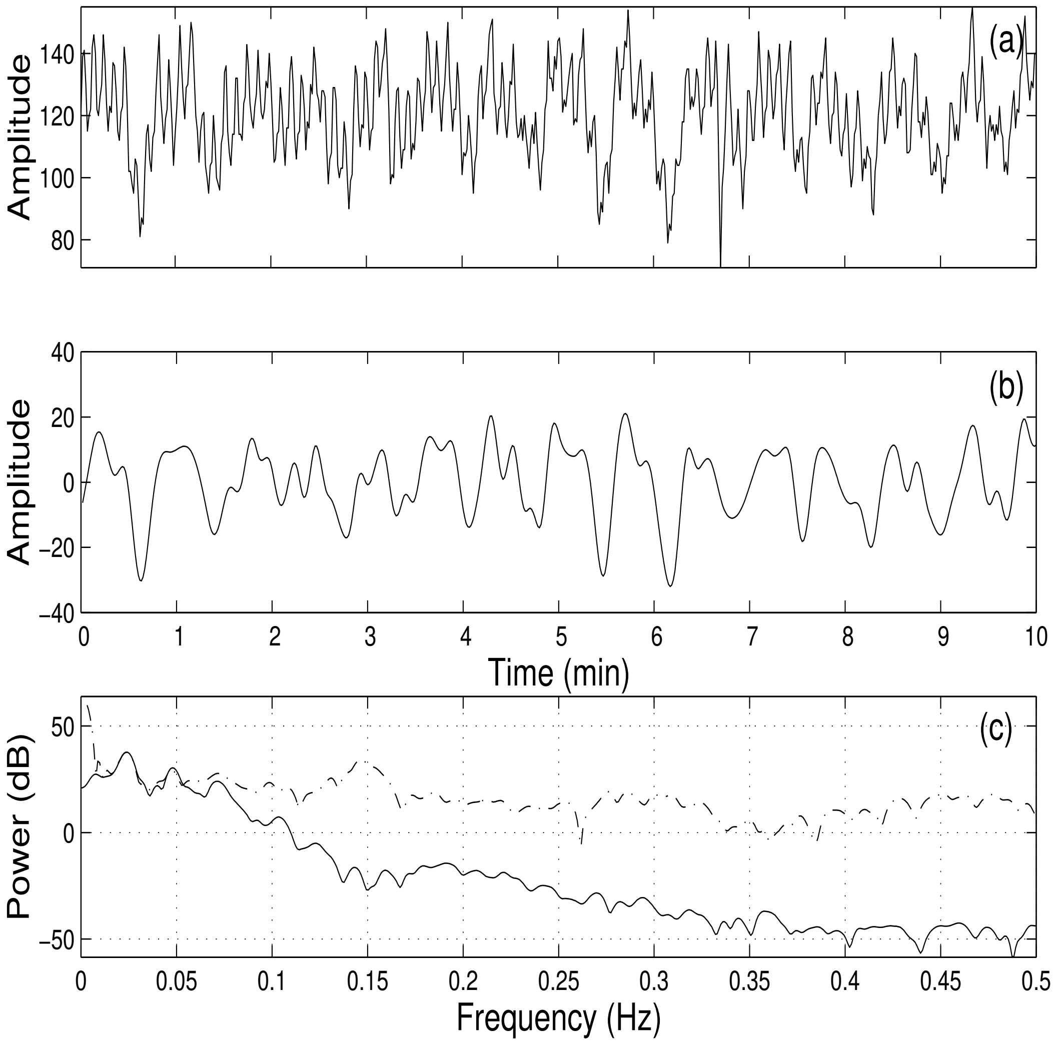

(a)
Amplitude
140
120
100
80
(b)
Amplitude
40
20
0
−20
−40
0
1
2
3
4
5
6
7
8
9
10
Time (min)
(c)
Power (dB)
50
0
−50
0
0.05
0.1
0.15
0.2
0.25
0.3
0.35
0.4
0.45
0.5
Frequency (Hz)


Figure 10

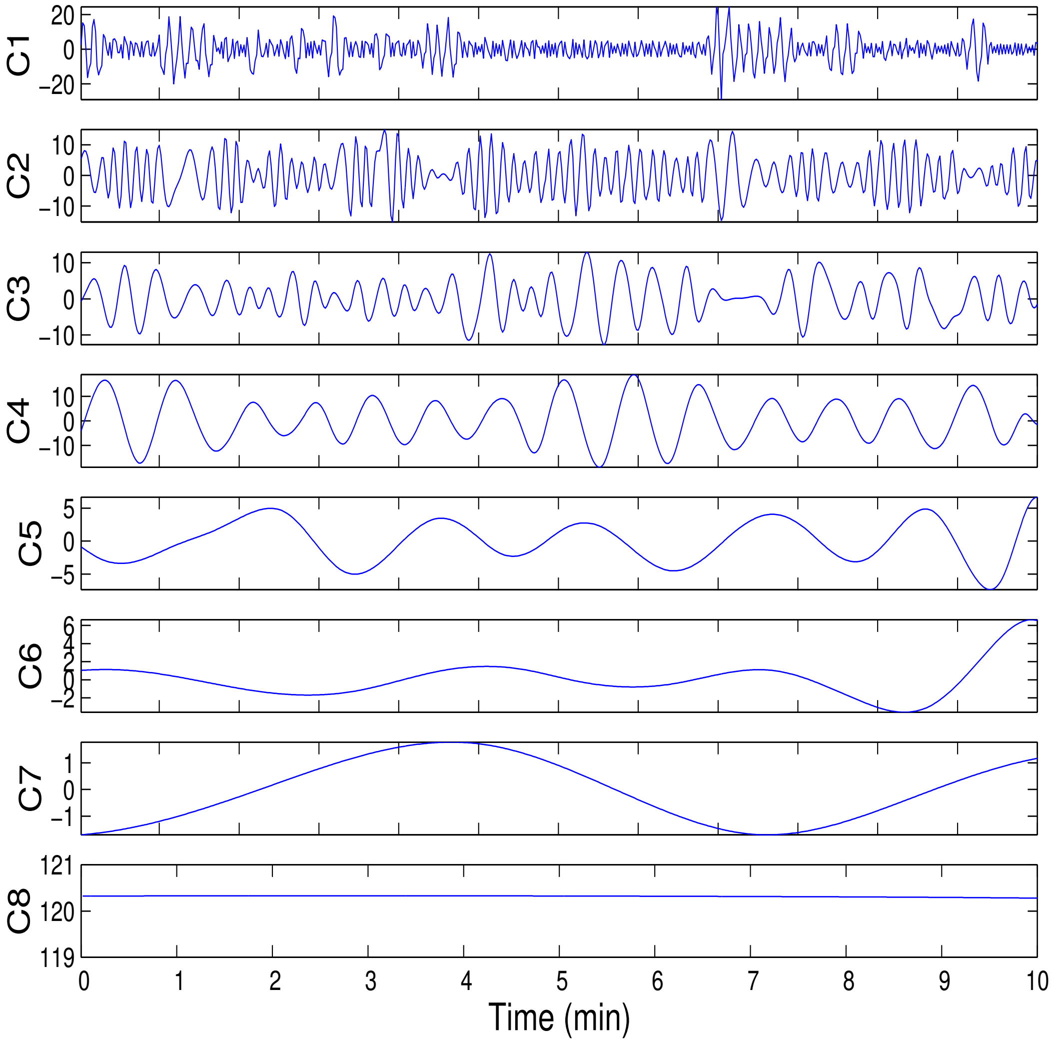
C1
20
0
−20
C2
10
0
−10
C3
10
0
−10
C4
10
0
−10
C5
5
0
−5
C6
6
4
2
0
−2
C7
1
0
−1
C8
121
120
119
0 1 2 3 4 5 6 7 8 9 10
Time (min)

Figure 11

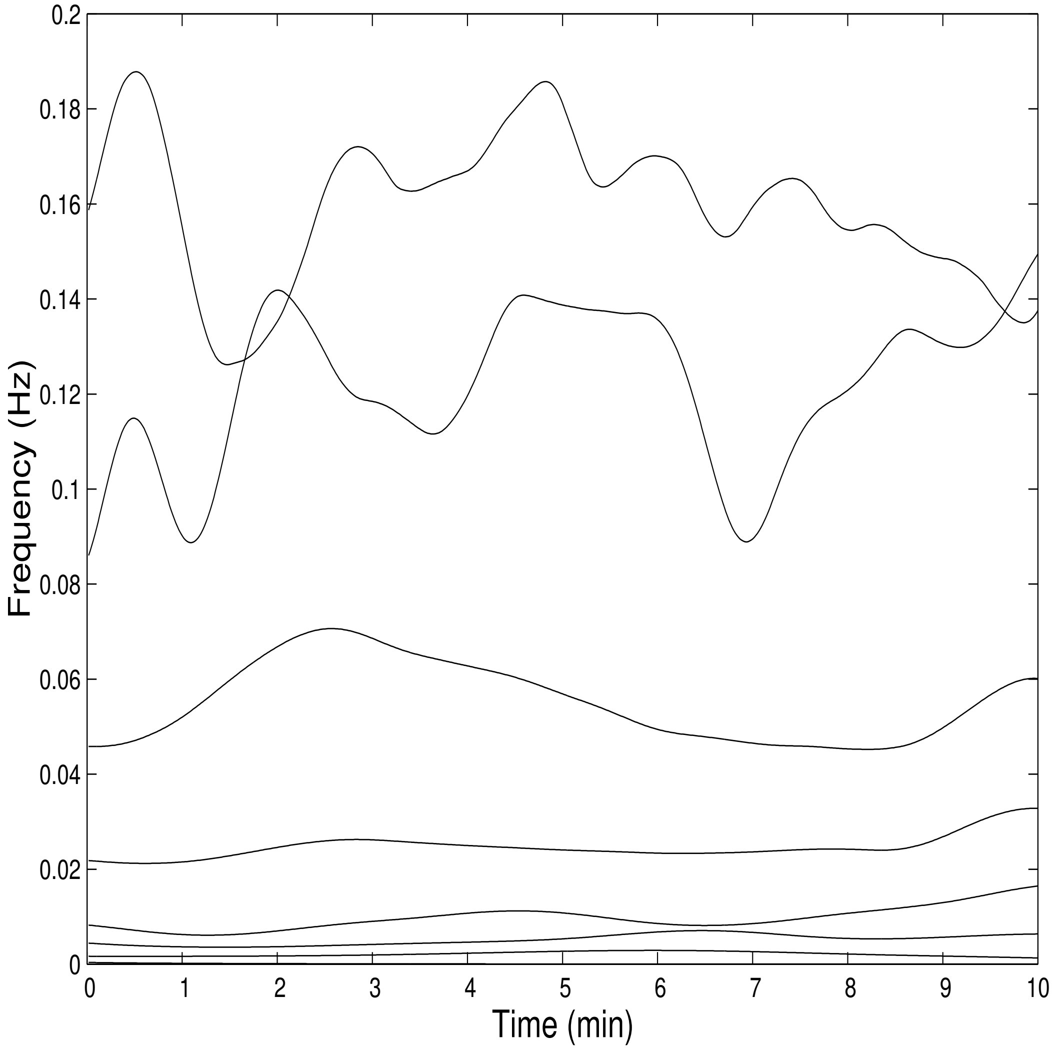
Frequency (Hz)
Time (min)
0.2
0.18
0.16
0.14
0.12
0.1
0.08
0.06
0.04
0.02
0
0 1 2 3 4 5 6 7 8 9 10

Figure 12

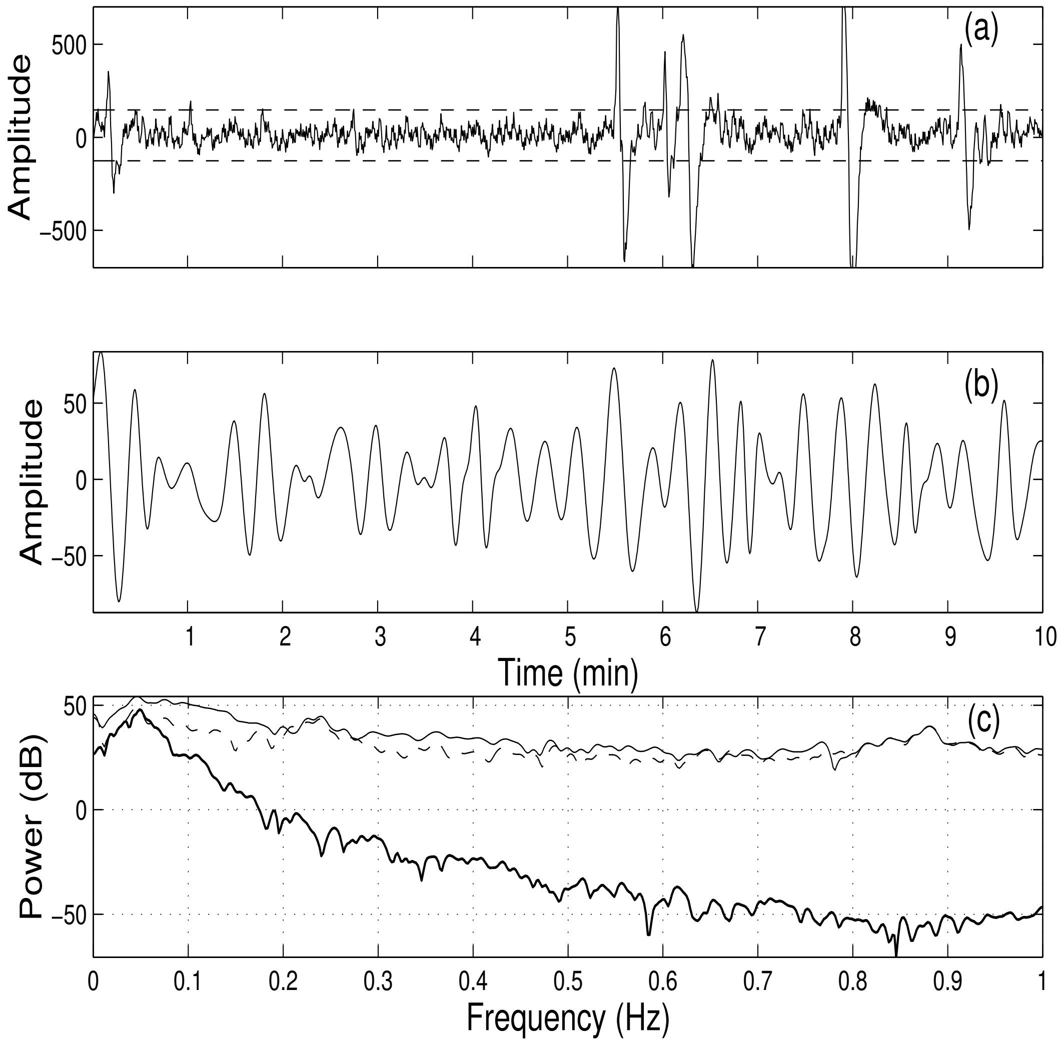
(a)
500
0
−500
Amplitude
(b)
50
0
−50
Amplitude
1
2
3
4
5
6
7
8
9
10
Time (min)
(c)
50
0
−50
Power (dB)
0
0.1
0.2
0.3
0.4
0.5
0.6
0.7
0.8
0.9
1
Frequency (Hz)

Figure 13

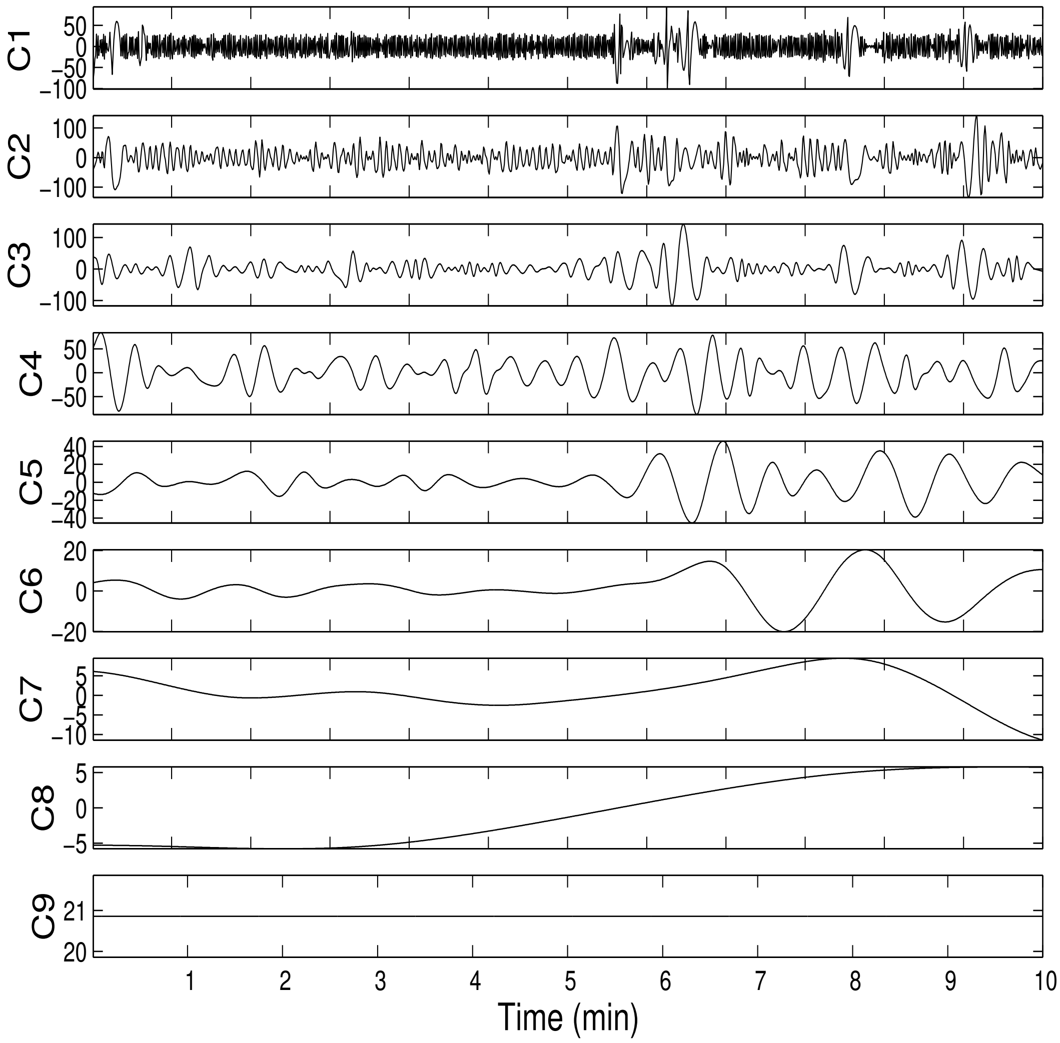


Figure 14